Photo-responsive lignin fragment-based polymers as switchable adhesives

Pallabi Sinha Roy, Matthieu Mention, Antonio Patti, Gil Garnier, Florent Allais, Kei Saito

Photo-responsive lignin fragment-based polymers as switchable adhesives

Pallabi Sinha Roy,[a,b] Matthieu M. Mention,[c] Antonio F. Patti,[a,b] Gil Garnier,*[b,c] Florent Allais*†[b,c] and Kei Saito*†[d]

Easy detachable and reusable adhesives are attractive as single-use adhesive replacements to reduce waste and promote reuse, recycling, or even upcycling options. Lignin, the second most abundant polymer and a byproduct of the paper-pulp industry, was utilized to design a novel, highly tunable reversible polymer adhesive. The approach adopted was to take advantage of the photo-responsive property of the α,β-unsaturated ester moiety of the *p*-hydroxycinnamic acid structure synthesized in this work using lignin-oxidation compounds and modified to attain reversible adhesion switching. The reversibility is achieved by the exposure of UV light that cleaves the covalent cyclobutane rings originally formed from α,β-unsaturated bond of the ester, which softens the material and makes it easily separable. The original polymer structure can be established again by recrosslinking to offer reworkability. The Design of Experiments (DoE) method was introduced to optimize the significant variables to achieve optimum lap shear strength for the adhesive. The effect of various structural aspects shows a high tunability of the structure to meet the property requirements. The design strategy of the polymer adhesive from renewable resources, along with the structure-property analysis mechanisms described in this work, can be implemented to engineer new bio-based and reusable adhesives.

1. Introduction

Lignin is a readily available and economical renewable resource, which is generated as a byproduct in the bioethanol and paper-pulp manufacturing processes and is widely considered as not efficiently used to its full potential.[1-2] Due to its aromatic structure and its capacity to replace petrochemicals, lignin has become a valuable biomass and has recently drawn considerable attention.[3] Most of this biopolymer is basically burnt to produce energy when it can be explored to synthesize many chemicals and polymers for high-value applications.[4] Lignin and lignin-derived compounds have significantly contributed to the recent advancement of sustainable polymers. High-value polymers, such as vitrimers, thermosets, thermoplastics, low-toxicity solvents and photo-responsive polymers, are some of the specialty areas where lignin and lignin-derived compounds have been explored.[5-8]

In recent years, photo-responsive polymers have gained significant popularity, as the light source can be applied to form the polymers in the solid state. This eliminates the usage of harmful solvents and the reversible material formed can be used multiple times only by controlling the irradiation using a light stimulus.[9-10] Most commonly, through [2+2] cycloaddition reaction, reversible unsaturated double bonds are converted to cyclobutane ring using UV light and the reverse reaction occurs when a different and higher energy UV light is applied.[11] Coumarin and cinnamic acid moieties can be utilized to produce photo-responsive polymers for several value-added applications, such as self-healing, photo-resist, liquid crystals and other smart materials.[12-14] Photo-reactive reusable adhesives are one such application area that can be very effective in repairing and recycling of polymer materials and reduce waste to an extent where conventional single-use adhesives fail.[15] Azo polymers have been explored to synthesize light-switchable adhesives using *cis-trans* photo-isomerization[16]. Both photo- and thermo-responsive dynamic covalent bonds have been utilized to prepare reversible adhesive by anthracene functionalization for underwater application.[17] Spiropyran photoisomerization has also been used to fabricate high glass transition temperature (T_g) polymer with reversible adhesion properties.[18] Grafted lignin has also produced reversible adhesives with self-healing ability.[19] Deconstructed lignin has been utilized to produce pressure-sensitive adhesives.[20-21] Lignin catechol chemistry has also been used with soybean protein to synthesize bio-based single-use adhesives.[22] Skin-adhesive sensor with self-healing capacity has unsaturated ester bonds using lignin-derived compounds to create highly tunable structures to match specific properties for reusable adhesive applications has not been significantly explored. The cinnamate structure generally displays low reversibility, however, these structures have also been proven to achieve the required properties for many applications, such as shape memory, mendable network polymer, sol-gel transitions, photonic films, nanoparticles with reversible size change properties, and so on.[24-30] The synthesis of tri- and tetra-functional structures using cinnamate moieties generated from lignin-derived compounds was carried out previously by our group for self-healing application.[31] Their properties were also systematically tuned and modified by structure-property analysis to reach the maximum possible reversibility suitable for the specific end-use.

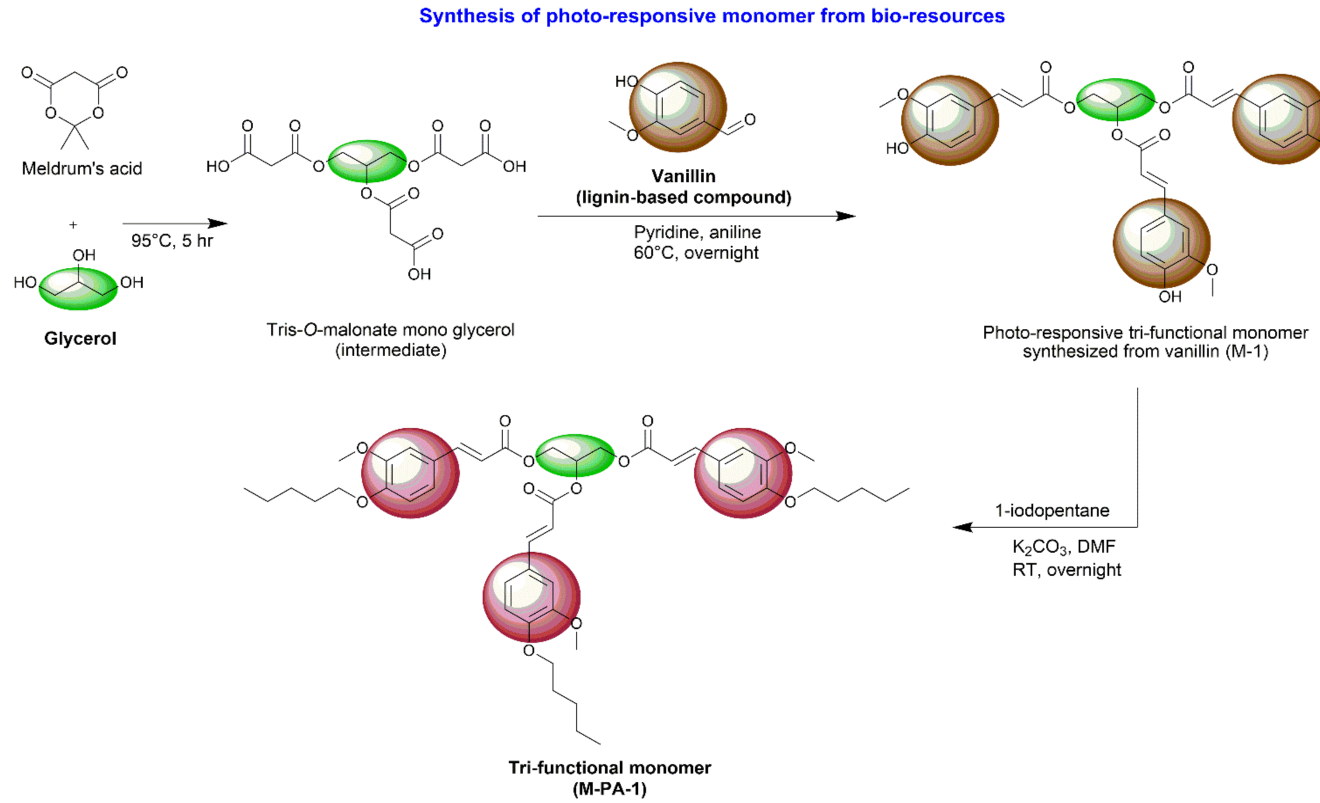

Scheme. 1 Synthesis of bio-based photo-responsive tri-functional monomer for reversible and reusable adhesive application.

been synthesized from lignin-grafted copolymers.[23] However, the synthesis of photo-responsive monomers by generating

This study presents the synthesis of reusable photo-responsive adhesives using bio-resources. Typically, [2+2] cycloaddition reactions can be applied in such applications, where balancing different properties is particularly important and fine-tuning of the required properties can be achieved by structure-property analysis.[31] The adhesive bonding and debonding process can be achieved by bond breaking and bond formation with the application of UV light. The monomers should have the proper viscosity to enable wetting and transport of the adhesive onto the substrate and be crosslinkable under UV light to provide polymers with optimum rigidity and strength to hold two substrates together.[16, 32] In addition, after breaking down into monomers or oligomers during decrosslinking, the material should become soft enough to detach from the substrate. The design aspect of the polymer adhesive is thus a critical factor. Here, multi-functional cinnamate-like monomers with unsaturated double bonds were synthesized using vanillin, a product of oxidative degradation of lignin, which is also commercially available; 3, 4-dihydroxybenzaldehyde, can be obtained via oxidative degradation followed by a demethylation process; and glycerol, a byproduct of the biodiesel production process.[33-37] The critical properties, such as the extent of crosslinking, decrosslinking, glass transition temperatures and their effect on adhesive lap shear strength, were analyzed for six different structures with tri-, tetra-, and hexa-functional core and catechol, methoxy, propyl, and pentyl side chain attachments. We hypothesized that, due to the inherent photo-reversible properties and the high tunability of the structures, we could potentially make the functional polymers work as reusable adhesives. As a result of the structure-property relationship study, multi-functional polymer adhesives were successfully synthesized with reusable properties. The main structural component of the reworkable adhesive is based on glycerol and vanillin; both can be derived from bio-resources, vegetable oils and wood, respectively. The tri-functional monomer structure was mainly designed in such a way so as to have the α,β-unsaturated ester bonds formed via the Knoevenagel–Doebner condensation reaction that can be converted to a polymeric structure by the application of UV light. The design, modifications and structure-property analysis to achieve reusable adhesive properties are unique to this research. Our novelty lies in the fact that the UV light-stimulated reversible and reusable polymer adhesive synthesized from vanillin and glycerol is a novel design that was purposefully functionalized with different side chains to achieve the required properties. This work thus can lead to a new generation of bio-based and reversible photo-responsive polymer adhesives with highly tunable structures and the structural analysis can provide a baseline for the synthesis of more engineerable bio-based adhesives in the future.

2. Results and discussion

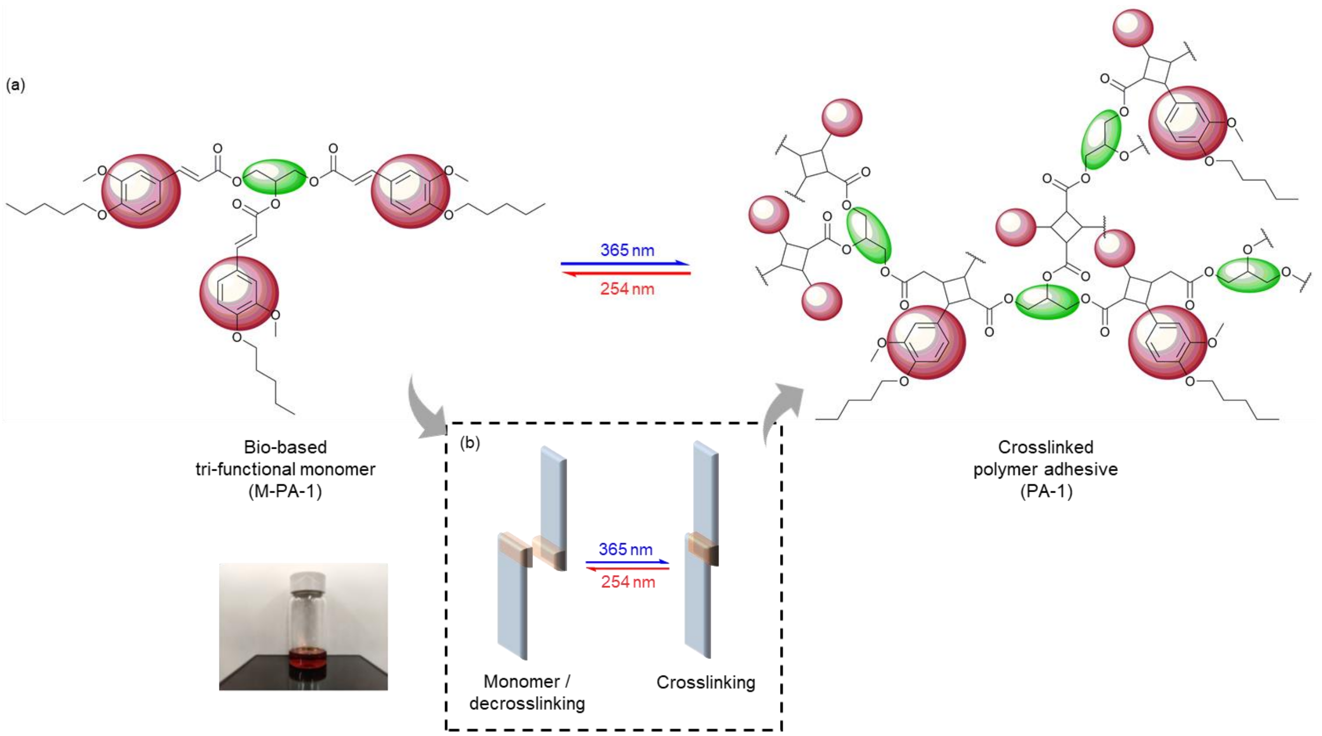

Figure. 1 Formation of crosslinked polymer network from tri-functional monomer (a) Conversion of the unsaturated ester bonds to cyclobutane rings and vice versa (b) Schematic illustration of photo-reversible adhesion upon irradiation at 365 nm and 254 nm.

2.1. Synthesis, design and analysis

The design of the reworkable adhesive is primarily based on the photo-responsive α,β-unsaturated ester moieties present in the cinnamate-based structures that can undergo [2+2] photocycloaddition reaction. Vanillin and 3, 4-dihydroxybenzaldehyde, two compounds that can be obtained from lignin, were used to synthesize multi-functional monomers with α,β-unsaturated ester moiety. The polymer was formed upon UV light irradiation at 365 nm. The backbone and the side chains of the monomers were purposefully modified to establish the structure-property relationship, particularly important for adhesive applications. Tri- and tetra-functional monomers were synthesized using glycerol and pentaerythritol as linkers, respectively. Another hexa-functional monomer was prepared using dipentaerythritol as a linker to comprehend the effect of multi-arm structure on the adhesive properties. Knoevenagel-Doebner condensation reaction, followed by a subsequent alkylation reaction, was employed to synthesize the monomers and treated under UV to create a crosslinked polymer network [Scheme 1, Figure 1]. Such properties of these cinnamate-based structures are due to the [2+2] photocycloaddition reaction, where the α,β-unsaturated ester bonds can be broken by using 365 nm UV light and cyclobutane rings are formed [Figure 1]. Higher energy UV can then be used to break the cyclobutane bonds and reform the α,β-unsaturated ester bonds. Such compounds can thus be used for photo-reversible applications. Williamson etherification was used to functionalize the phenolic group and attach longer alkyl chains to provide enough flexibility to the structure to make it suitable to work as adhesives. Optimization of the variables was especially important to achieve proper adhesion strength. A higher amount of material requires higher UV radiation to crosslink to provide the required adhesion strength; however, longer radiation time increases the crosslinking making it brittle.

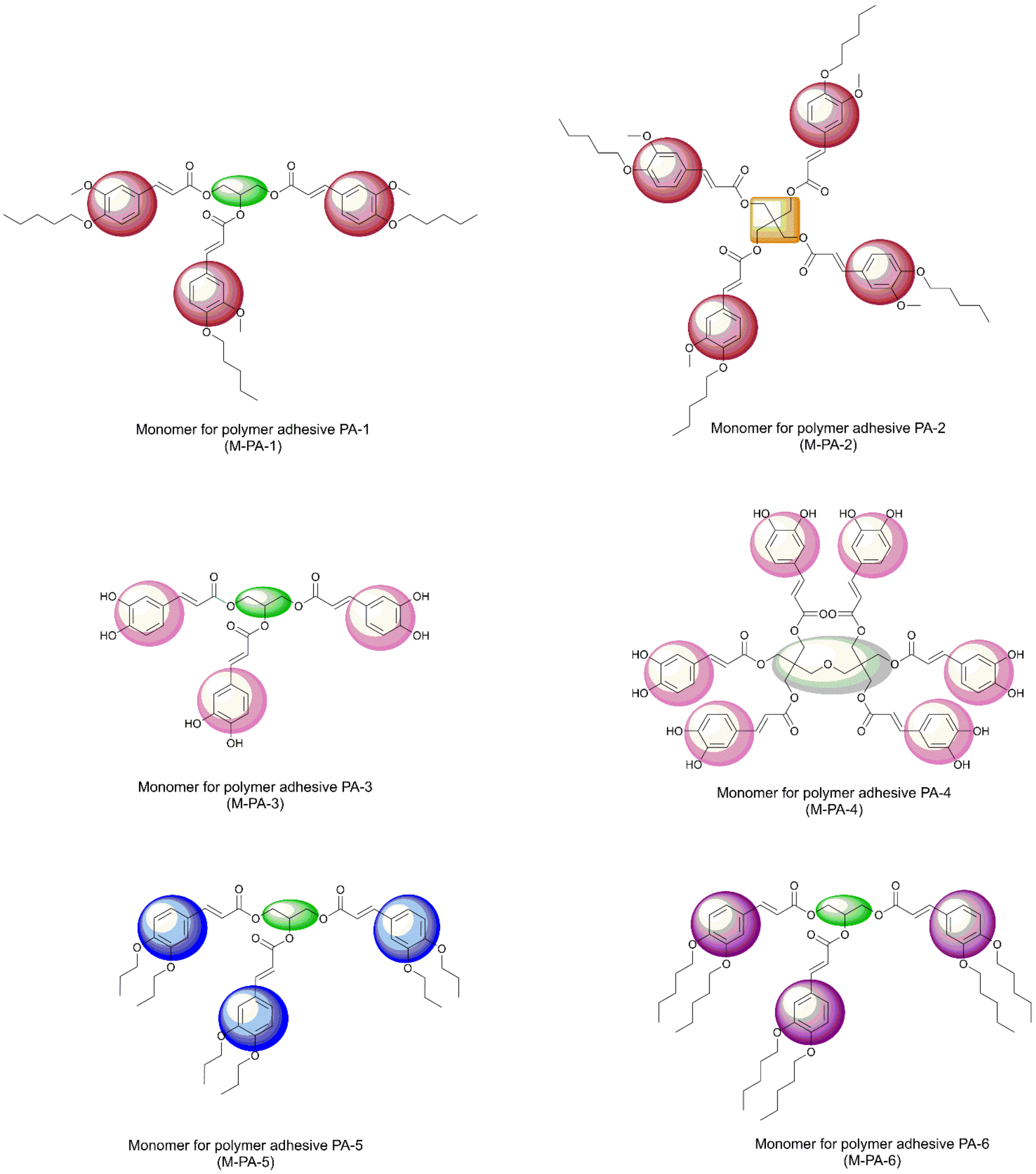

Figure. 2 Different structures considered for structure-property relationship study.

In addition, the higher the molar concentration, the higher the inter- and intra-molecular crosslinking, thus making it more difficult to separate the substrates to use as a reworkable adhesive. This is why a Design of Experiments (DoE) was used to optimize the variables and reach the maximum possible adhesion strength with reversible properties. Along with this, the analysis provided an indication of the predictability and reproducibility of the obtained results. Failure mode analysis was also carried out to understand the mechanism of failure (adhesive failure, cohesive failure, or substrate failure), to minimize the causes and to improve the design by structural modification.

2.2. Structure and property analysis

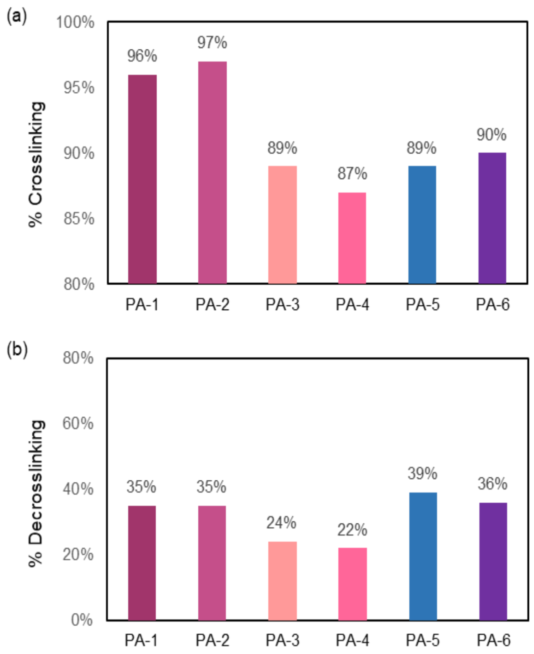

Figure. 3 Property comparison of the different structures (a) crosslinking % upon irradiation at 365 nm (b) decrosslinking % upon irradiation at 254 nm.

It is well-known that adhesion is a complex phenomenon that depends on multiple mechanisms and factors.[38-39] One of those is mechanical interlocking, i.e., the flow of the adhesive on the surface of the substrate followed by hardening causes interlocking. Another is diffusion which occurs between two polymers, primarily by chain entanglement. Other forces include physical bonding, like van der Waals forces, and chemical bonding, such as covalent and ionic bond formation. Therefore, adhesion forces are also dependent on several aspects, such as the chemical composition of the substrate and the adhesive, their compatibility, surface roughness, and cleanliness (i.e., absence of contaminants). The basic requirement for a material to perform as an adhesive is that it first wets and, if possible, spreads well on the surface of the substrate. It should be a viscous fluid that subsequently becomes solid to achieve sufficient strength to retain two surfaces attached to each other. To understand the structural aspects of the lignin-derived monomers used in this study and their effect on adhesion performance, a systematic structure and property analysis was conducted. Three different linkers and four different functional attachments were considered for this study and the property assessment was carried out to evaluate the toughening of the polymer adhesive material upon crosslinking under UV light [Figure 2]. The photo-responsive properties, such as crosslinking and decrosslinking extent, thermal properties, for instance, the degradation and the glass transition temperature, and the lap shear strength of these structures were evaluated to determine the effect of the structural aspect on adhesion strength.

The crosslinking and decrosslinking properties of the compounds were measured by UV-Vis spectroscopy. The peak at 327 nm corresponds to the α, β-unsaturated ester bond. As the bonds break upon irradiation at 365 nm UV light, the absorbance peak starts to decrease; reverse phenomena are observed when irradiated at 254 nm of UV [Figure S10 to S15]. Almost all the compounds show 87-97% crosslinking, which provides the material adequate strength to adhere, while the attained extent of decrosslinking, which is 22 to 39%, provides sufficient detachment points by breaking a portion of the cyclobutane bonds [Figure 3a and 3b]. Tri- and tetra-functional PA-1 an d PA-2 polymer adhesives provided the higher crosslinking, 96% and 97%, respectively [Figure S10a & S11a], while the hexa-arm compound PA-4 offered only 87% crosslinking [Figure S13a], possibly due to the structural rigidity and difficulty in the accessibility of the unsaturated double bonds to form the dimers. The structural rigidity of the tri-arm monomers without alkyl modification restricts the crosslinking to 89% or below (PA-3 and PA-4); with alkyl chain modification, it is mostly 90% or above (PA-1, PA-2 and PA-6). The decrosslinking extent is also lower in catechol-containing polymers, 22-24% (Figure S12b and S13b), as they might form radicals (under higher energy UV light) that attack the double bonds formed during decrosslinking.[40-41] When phenolic -OH groups were replaced with methyl or longer alkyl chains, the decrosslinking extent increased to 35% or above (Figure S10b and S11b). As mentioned earlier, the cinnamate structure shows limited reversibility. This phenomenon has previously been investigated by researchers and a number of reasons could account for the limited reversibility that has been reported. The low quantum yield for dimerization is one of the main reasons for the low reversibility of the cinnamate-based structures; the reversibility is mostly limited in the solid state

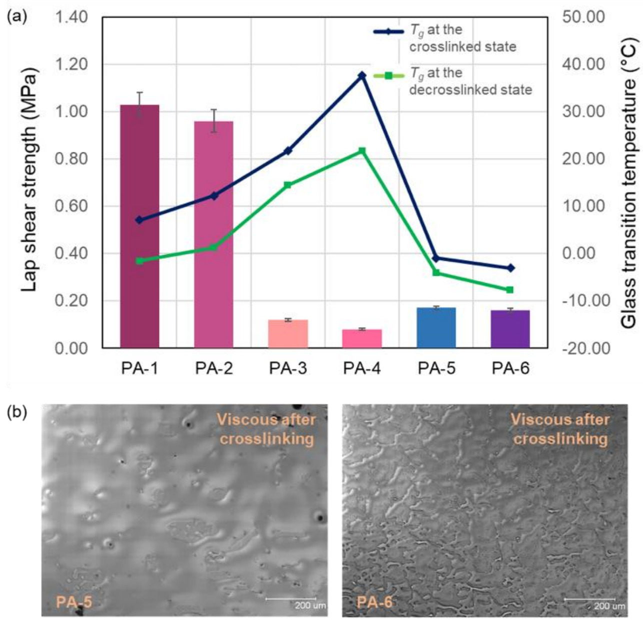

Figure. 4 (a) Comparison of lap shear strength and glass transition temperature at crosslinked and decrosslinked state (b) Optical microscopic images of PA-5 and PA-6 after crosslinking (images taken after lap shear test).

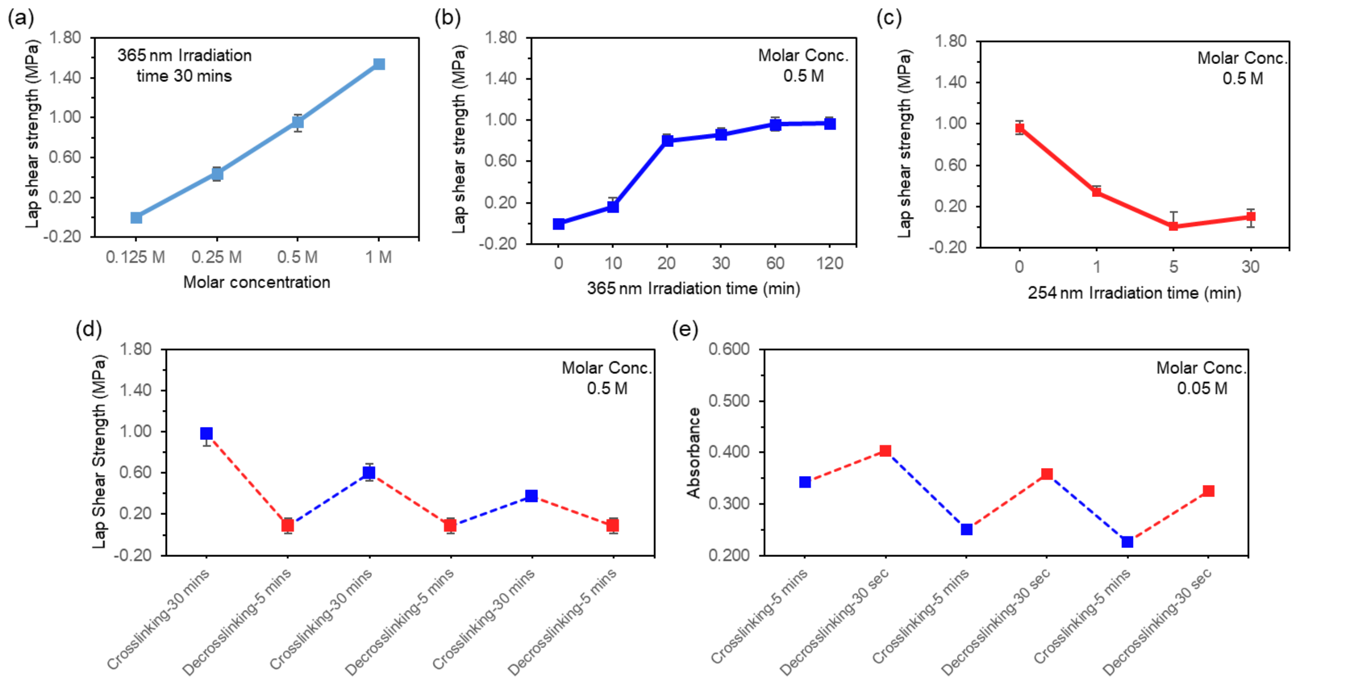

Figure. 5 Lap shear strength of the polymer adhesive PA-1 with respect to variables - (a) molar concentration (b) 365 nm irradiation time (c) 254 nm irradiation time (d) reversibility cycle and (e) reversibility cycle with respect to absorbance from UV-Vis spectrometer.

and a higher rate of dimerization occurs in the fluid medium.[25, 42] The formation of *cis-trans* configuration also could contribute to the lower values of photo-reversibility, as the extinction coefficient of the *trans* isomer is higher than the *cis* one, which means the *trans* shows a lower absorbance.[25, 30] The extent of reversibility, which is calculated from the absorbance value of the UV light, could thus be affected by the formation of *cis-trans* configuration apparently showing lower values than the actual reversibility. The power of the UV reactor might also affect the reversibility values.[26] Furthermore, photo-oxidation in air upon exposure to UV light reduces the reversibility to some extent, and the reversibility values are, therefore, higher in the nitrogen atmosphere.[31] However, the limited reversibility was suitable for many different applications and hence, it was not a significant concern here. Figure S16 shows the comparative chart for the degree of crosslinking with respect to 365 nm irradiation time for all the compounds and it can be seen that, for PA-1 and PA-2, a sharp increase in the extent of crosslinking can be observed up to 120 minutes and beyond that the crosslinking percentage becomes almost constant. For all other compounds, around 180 minutes is required to attain the maximum crosslinking. Figure S17 summarizes the comparison of 254 nm irradiation time and the time at which maximum decrosslinking is observed. This chart also shows that PA-1 and PA-2 were the fastest to attain the maximum decrosslinking extent, 35% at 2 minutes. The Fourier-transform infrared (FTIR) spectra of PA-1 were analyzed to observe the pattern of crosslinking and decrosslinking [Figure S9]. A shift in the carbonyl peak at 1708 cm^{-1} to 1719 cm^{-1} was observed after crosslinking, as the environment of this functional group changes with the breaking of the ester bond and the formation of the cyclobutane ring. The change in the position of this peak was recorded after decrosslinking when it moved back to 1709 cm^{-1} again.

The thermal properties of the polymeric materials were characterized by thermogravimetric analysis (TGA) and differential scanning calorimetry (DSC). The TGA plot for all the compounds shows that they are thermally stable up to 180-200 °C [Figure S18 to S23]. DSC was used to obtain the glass transition temperature of the polymer, which is a critical parameter for the evaluation of the adhesion strength. Figure 4a illustrates the comparison of lap shear strength with the glass transition temperature. PA-1 and PA-2 were viscous liquids in the monomer state at room temperature and subsequently became solid after crosslinking under 365 nm UV irradiation, providing enough strength to reach a lap shear value of around 1 MPa. The glass transition temperatures of PA-1 and PA-2 in the crosslinked state were 7 °C and 12 °C, respectively [Figure S24 and S26]. The catechol-containing compounds PA-3 and PA-4 were solid in the monomer state and not suitable for providing proper wetting of the substrate; their crosslinked T_gs are 21 °C and 38 °C, respectively [Figure S28 and S30]. PA-6 and PA-7 were liquid at room temperature and remained viscous even after crosslinking and hence, cannot offer sufficient adhesive strength [Figure 4b]. The glass transition temperature of the polymer adhesives PA-1 to PA-6 in the decrosslinked state were -1 °C, 1 °C, 14 °C, 21 °C, -4 °C and -7 °C, respectively [Figure S25, S27, S29, S31, S33 and S35]. The decrease in T_g after

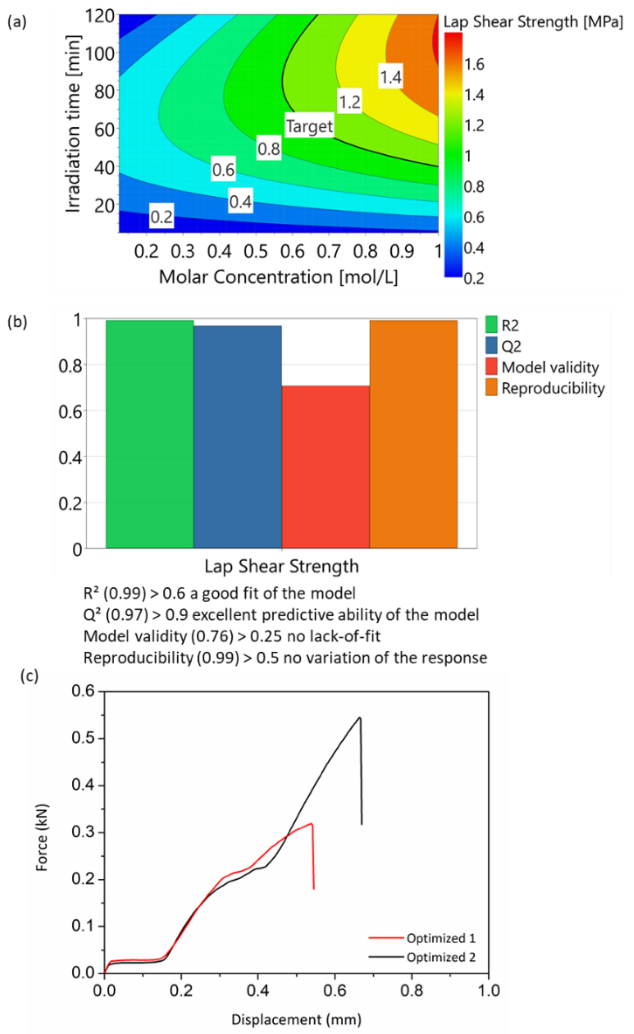

Figure. 6 (a) Response surface for the lap shear strength (b) the summary of fit for the developed model (c) Force-displacement curve for the optimized conditions.

decrosslinking as shown in Figure 4a is due to the partial photocleavage of the polymer adhesive to oligomers or monomers.

From the aforementioned observations, it is obvious that glycerol and pentaerythritol linkers were efficient to form proper crosslinked structures, while the dipentaerythritol linker displayed an accessibility issue for the dimerization. Phenolic -OH groups replaced with one methyl and one pentyl chain offered sufficient structural flexibility to form a viscous liquid suitable for adhesives, while two propyl and two pentyl chains contributed to even higher flexibility; however, these were not optimum for this specific application. The tri-functional polymer adhesive PA-1 showed highest adhesion strength and was hence selected for further study on adhesion strength and optimization.

2.3. Adhesion performance evaluation and optimization

The adhesion performance of the tri-functional polymer adhesive PA-1, synthesized from glycerol and vanillin, was assessed statistically and optimized with respect to critical variables, such as molar concentration, 365 nm irradiation time for crosslinking, 254 nm irradiation time for decrosslinking and reversibility. The reversibility cycle was also assessed to establish the reworkability of the adhesive material and compared with the absorbance spectra from the UV-Vis spectrometer.

The effect of molar concentration has an obvious effect on the strength of the adhesive material. As the molar concentration increases, the lap shear also increases as more structural units are available to crosslink within the same cross-sectional area [Figure 5a]. Up to 1 M concentration was used as this was able to provide adhesive strength of 1-1.5 MPa. Generally, lap shear strength of 1 MPa and higher is considered as high adhesion as per the literature.[43] Higher than 1 M concentration provided higher strength but lower reversibility, and the adhesion strength did not go back to 0-0.1 MPa upon decrosslinking and still offered an adhesion strength of ~ 0.5 MPa after 30 minutes of irradiation [Figure S36].

The irradiation time under 365 nm UV light was also varied to assess the effect of crosslinking on the adhesive strength at 0.5 M concentration [Figure 5b]. Irradiation time of up to 10 minutes was not sufficient to provide proper adhesion strength, whereas a sharp increase in the strength was observed after 20 minutes of irradiation. Beyond, almost constant strength was achieved, which indicates the maximum limit of the adhesive material (at a particular concentration). Upon further increase in irradiation time, the strength decreases, probably because of the formation of a brittle solid crosslinked structure. Hence, optimizing the concentration with the 365 nm irradiation time was specifically important to achieve the maximum possible strength for a particular structure.

The reversibility of the crosslinked polymer under higher energy UV light is another important aspect to be considered as a dismantlable and reworkable adhesive. Irradiation for 1 minute showed a sharp decrease in strength, while after 5 minutes of irradiation, the strength becomes negligible, which means the substrates can be separated easily from each other [Figure 5c]. The reversibility cycle is critical for the performance of an adhesive for multiple use and reprocess ability. The adhesion strength and the UV-Vis absorbance data were used to assess the reversibility cycle. 0.5 M concentration was used for lap shear strength comparison, while 0.05 M concentration was used to record the UV-Vis spectra as clear absorbance peaks cannot be obtained at a higher concentration. Figures 5d and 5e clearly demonstrate that this adhesive can be used multiple times, providing adhesion even after three cycles. However, Figures 5d and 5e cannot be accurately correlated at

Table 1 Independent variables used for the design.

Name	Abbr.	Units	Type	Settings	Precision
Molar concentration	Mol	mol/L	Quantitative	0.125 to 1	0.0219
Irradiation time	Irr	min	Quantitative	5 to 120	2.88

the chemical level as two different molar concentrations have been used. The trends shown in these two figures are presented to verify that reversibility can be achieved for multiple cycles.

The Design of Experiments (DoE) was introduced to identify the optimum conditions for the tri-functional material to achieve the highest possible adhesive strength and reusability at the same time. Response surface methodology (RSM) is a statistical tool that is commonly used for DoE analysis, model building and optimization.[44] It helps to understand the effect of individual variables as well as the collective effect of multiple variables on the response value using less experimental conditions. Here, RSM was employed to build the model using the two input variables: molar concentration and irradiation time. The upper and lower values of the two inputs for the optimization study were determined from the initial sets of adhesion data. The response, which was lap shear strength, was captured against the model input values; finally, optimization was performed using the benchmark value from the literature.[43] The range of input variables used in the software was [-1 (min. value): 0.125 M and 5 min; +1 (max. value): 1 M and 120 min] given in Table 1. A total of 14 experiments were performed as provided by the design model [Table S1].

The initial evaluation of the experimental values identified two outliers that were excluded from the computational analysis (entries 5 & 6, Table S1); hence, the number of experiments considered for the study was N=12. The RSM chart was created to plot the effect of input variables on the response value [Figure 6a]. The D-optimal coefficients of the quadratic model were evaluated to determine the direct influence of input variables on the response values and the interaction between the variables by square terms (Mol*Mol) and (Irr*Irr), and quadratic term (Mol*Irr) [Figure S37]. The model shows that independent input variables have a positive impact on the response value. The square term (Mol*Mol) is non-significant in our case and a negative impact has been observed for (Irr*Irr). The quadratic term, evaluating the interaction between variables, has a positive contribution to the output.

From the summary of fit, it was observed that the value of R^2 was 0.99, which shows a good fit of the model, while the Q^2 with a value of 0.97 demonstrates excellent predictability [Table S2]. The model validity was 0.76 (> 0.25), which indicates no lack of fit and the reproducibility value was 0.99, which illustrates excellent reproducibility [Figure 6b]. Moreover, the analysis of the variance confirmed the significance of the model statistically ($p < 0.05$) and a similar magnitude of replicate errors, i.e., no lack of fit ($p > 0.05$). Two optimal conditions were predicted by the model. The first one is to reach a lap shear strength of 1 MPa, which is set as the target according to the literature[43]; the second condition is to achieve the maximum strength possible with the model. Experiments were performed on the optimization conditions to evaluate the model predictability and the results are given in Table 2. Figure 6c displays the force-displacement curve for the two optimized conditions. A maximum of 1.74 MPa strength was achieved with our system, which was comparable or higher than most of the UV-switchable adhesives.[16, 43, 45]

Equation of the model:

$$Y = 0.9222 + 0.4319(Mol) + 0.3518(Irr) - 0.4682(Irr*Irr) + 0.3629(Mol*Irr)$$

2.4. Failure mode analysis

The mode of failure for all the structures was assessed visually by an optical microscope [Figure S39]. The glass transition temperature of the polymers can be considered for the explanation of such failure mode. PA-1 and PA-2, which provide the best adhesion performances, have localized cohesive failure. On the other hand, PA-6 and PA-7, whose glass transition temperatures are below 0 °C after crosslinking, show the materials remain viscous even after crosslinking and thus cannot achieve good adhesion. Catechol-based structures PA-3 and PA-4 have higher glass transition temperatures and therefore became brittle after crosslinking and showed cohesive failure. For all the structures, the failure type was cohesive; no adhesive mode of failure was observed with this system. Hence, a balance between the viscosity of the material during application and rigidity after crosslinking was necessary to make a performant polymer adhesive material with optimum strength, which was successfully achieved with our designed structure and structure-property analysis.

3. Conclusion

A novel family of photo-reversible and reusable adhesives was designed from biomass-derived molecules. These adhesives are crosslinked polymers made from multi-functional cores and catechol, methoxy and alkyl side chain attachments. A series of tri-, tetra- and hexa- core monomers were synthesized and crosslinked into adhesive polymers by UV exposure. Their structures were engineered to achieve a fine balance between the main characteristics of the adhesive using a structure-activity analysis study. Among the monomers synthesized, the adhesion strength of the glycerol and vanillin-based tri-functional monomer was optimized to reach 1.74 MPa using a

Table 2 Optimal conditions predicted by the model and the final experimental values.

Conditions	Molar concentration (mol/L)	Irradiation time (min)	Predicted lap shear strength (MPa)	Experimental lap shear strength (MPa)
Optimized 1	0.57	89	1.00	1.02
Optimized 2	1.00	107	1.62	1.74

Design of Experiments, which is considered as high adhesion strength (defined as > 1 MPa) and is higher than most of the UV-reversible adhesives presently found in the literature. The lignin-based photo-reversible polymer adhesive can be used multiple times, thereby reducing waste generation and enabling possibilities of reuse and recycling. This study also provides the synthesis, mechanism and methods to optimize the structure-property of lignin-based switchable functional polymers for adhesive applications.

Experimental

Materials

Meldrum's acid, vanillin, 3,4-dihydroxybenzaldehyde, pentaerythritol, dipentaerythritol, iodopropane, iodopentane, aniline, K_2CO_3, $NaHCO_3$, silica gel (for column chromatography) and anhydrous $MgSO_4$ were purchased from Sigma Aldrich. Glycerol, concentrated HCl and all solvents were purchased from Thermo Fisher Scientific. All chemicals were used directly without purification.

Characterization

^{1}H NMR spectra were recorded on a Bruker DRK 400 (400 MHz) and were calibrated with DMSO-d_6 protons signals at δ 2.50 ppm. All data are reported as follows: chemical shift (δ ppm), multiplicity (s=singlet, d=doublet, t=triplet, quint=quintet, sext=sextet, dd=doublet of doublets and m=multiplet), integration, coupling constant (Hz) and assignment. ^{13}C NMR was recorded on the same Bruker DRK 400 and was calibrated with DMSO-d_6 signals δ 39.52 ppm. All data are reported as follows: chemical shift (δ ppm) and assignment. Photoreactions were carried out in UVP UV crosslinkers CL-1000L 365 nm and CL-1000 254 nm. FTIR and UV spectra were recorded using Agilent Cary 630 FTIR spectrometers and Shimadzu UV-1800 spectrometer, respectively. Differential scanning calorimetry (DSC) analysis and thermogravimetric analysis (TGA) were carried out using PerkinElmer DSC8000 and Mettler TGA/DSC1 STAR system, respectively. The maximum tensile force was measured using Instron 5566 Tensile Tester with a constant rate of 10 mm/min. Optical microscopic images were captured on an Olympus GX51 microscope. The Design of Experiments was generated using Modde v.12.0 software (Umetrics AB, Sweden).

For FTIR and UV-Vis analysis, the samples were prepared by dissolving the monomers in ethyl acetate (0.5M and 0.05M, respectively), followed by film formation on small square quartz slides using a spin-coater (30µL solution was used for the coating). The slide with 0.05M coating was placed on a quartz slide holder, and the absorbance was measured using a UV-Vis spectrometer at different timeframes, as shown in Figures S16 and S17. The FTIR measurement was carried out at monomer state, after crosslinking for 30 minutes and after decrosslinking for 5 minutes. For DSC and TGA study, drop casted samples on glass slides with 0.5M concentration in ethyl acetate were used (30µL solution was used), which were air-dried inside the fume hood for two hours before placing them inside the UV reactor. For crosslinking 365 nm wavelength and for decrosslinking 254 nm wavelength was used. For adhesive strength measurements, glass and quartz slides were used as substrates; quartz slides were used for reversibility studies. The adhesive was spin-coated with 100µL solution of different concentrations over the area of 312.5 mm^2 (12.5 mm x 25 mm) by covering the rest of the area of the slide with masking tape. After the coating, the masking tape was removed and the coated area was overlapped with another slide as shown in Figure 1b. The maximum force was measured using Instron tensile tester and the lap shear strength was calculated in MPa by dividing the maximum force with the area of the coating.

Synthetic procedures

Synthesis of tris-*O*-malonate mono glycerol (intermediate compound for tri-functional monomers M-PA-1, M-PA-3, M-PA-5 and M-PA-6). Glycerol (1 eq., 1.96 g, 21.3 mmol) and Meldrum's acid (3 eq., 9.21 g, 63.9 mmol) were stirred together in a round-bottom flask at 95 °C for 5 hours. After cooling at room temperature, the mixture was diluted in ethyl acetate and washed with saturated $NaHCO_3$ aqueous solution. The aqueous layer was then acidified with concentrated HCl until pH 1. It was then extracted again with ethyl acetate and the organic layer was dried over anhydrous $MgSO_4$, filtered and concentrated *in vacuo* to afford the desired intermediate as a pale-yellow oil (5.45 g, 15.6 mmol, 73%) which can be used without further purification. ^{1}H NMR (DMSO-d_6): δ (ppm) 3.40 (m, 6H, H2), 4.26 (m, 4H, H4), 5.23 (quint, 1H, J = 4.5 Hz, H5), 12.84 (s, 3H, OH); ^{13}C NMR (DMSO-d_6): δ (ppm) 41.3 (C2), 41.4 (C2), 62.3 (C4), 69.2 (C5), 166.4 (C3), 166.7 (C3), 167.8 (C1), 167.9 (C1).

Synthesis of tetra-*O*-malonate mono pentaerythritol (intermediate compound for tetra-functional monomer M-PA-2). Pentaerythritol (1 eq., 2.09 g, 15.4 mmol) and Meldrum's acid (4 eq., 8.69 g, 61.6 mmol) were stirred together in a round-bottom flask at 95 °C for 5 hours. After cooling at room temperature, the mixture was diluted in ethyl acetate and washed with saturated $NaHCO_3$ aqueous solution. The aqueous layer was then acidified with concentrated HCl until pH 1. It was then extracted again with ethyl acetate and the organic layer was dried over anhydrous $MgSO_4$, filtered and concentrated *in vacuo* to afford the desired intermediate as an orange oil (4.87g, 10.1 mmol, 66%) which can be used without further purification. ^{1}H NMR (DMSO-d_6): δ (ppm) 3.42 (s, 8H, H2), 4.14 (s, 8H, H4), 12.83; ^{13}C NMR (DMSO-d_6): δ (ppm) 41.3 (C2), 42.0 (C5), 62.8 (C4), 166.6 (C3), 168.0 (C1).

Synthesis of tetra-*O*-malonate dipentaerythritol (intermediate compound for hexa-functional monomer M-PA-4). Dientaerythritol (1 eq., 2.54 g, 10 mmol) and Meldrum's acid (6 eq., 8.65 g, 60 mmol) were stirred together in a round-bottom flask at 95 °C for 5 hours. After cooling at room temperature, the mixture was diluted in ethyl acetate and washed with saturated $NaHCO_3$ aqueous solution. The aqueous layer was then acidified with concentrated HCl until pH 1. It was then extracted again with ethyl acetate and the organic layer was dried over anhydrous $MgSO_4$, filtered and concentrated *in* *vacuo* to afford the desired intermediate as an orange oil (5.26 g, 6.8 mmol, 68%) which can be used without further purification.

Synthesis of tri-functional monomer M-1 using vanillin (second intermediate for M-PA-1, M-PA-5 and M-PA-6). Tris-*O*-malonate mono glycerol (1eq., 5.22 g, 14.9 mmol), vanillin (3 eq., 6.81 g, 44.7 mmol), aniline (0.3 eq., 411.8 μL, 4.47 mmol) were dissolved in pyridine and stirred together at 60 °C overnight. The reaction mixture was extracted with ethyl acetate (50 mL) and HCl 1M (50 mL), the organic layer was dried over anhydrous $MgSO_4$, filtered and concentrated *in vacuo*. The crude product was then purified by column chromatography using ethyl acetate/cyclohexane (50/50) as an eluant to afford M-1 monomer (7.92 g, 12.8 mmol, 86%). ^{1}H NMR (DMSO-d_6): δ (ppm) 3.79 (s, 9H, H10), 4.42 (m, 4H, H11), 5.45 (m, 1H, H12), 6.51 (d, 2H, J = 15.9 Hz, H2), 6.53 (d, 1H, J = 15.9 Hz, H2), 6.77 (d, 3H, J = 8.1 Hz, H6), 7.11 (dd, 3H, J = 8.3, 1.7 Hz, H5), 7.33 (d, 3H, J = 1.9 Hz, H9), 7.57 (d, 3H, J = 15.8 Hz, H3), 7.59 (d, 1H, J = 15.8 Hz, H3), 9.65 (s, 3H, OH); ^{13}C NMR (DMSO-d_6): δ (ppm) 55.7 (C10), 59.8 (C11), 66.9 (C12), 111.1 (C9), 113.7 (C2), 115.5 (C6), 123.5 (C5), 125.4 (C4), 145.9 (C3), 148.0 (C8), 149.5 (C7), 166.4 (C1).

Synthesis of intermediate tetra-functional monomer M-2 using vanillin (second intermediate for M-PA-2). Tetra-*O*-malonate mono pentaerythritol (1eq., 0.53 g, 1.1 mmol), vanillin (4 eq., 0.67 g, 4.4 mmol), aniline (0.4 eq., 39.3 μL, 0.44 mmol) were dissolved in pyridine and stirred at 60 °C overnight. The reaction mixture was extracted with ethyl acetate (10 mL) and HCl 1M (10 mL), the organic layer was dried over anhydrous $MgSO_4$, filtered and concentrated *in vacuo*. The crude product was purified by column chromatography using ethyl acetate/cyclohexane (70/30) as an eluant to afford M-2 monomer (0.84 g, 1 mmol, 91% yield). ^{1}H NMR (DMSO-d_6): δ (ppm) 3.77 (s, 12H, H10), 4.29 (m, 8H, H11), 4.99 (m, 1H, H12), 6.47 (d, 2H, J = 15.8 Hz, H2), 6.51 (d, 2H, J = 15.8 Hz, H2), 6.74 (d, 4H, J = 8.9 Hz, H6), 7.08 (d, 4H, J = 7.1 Hz, H5), 7.30 (s, 4H, H9), 7.56 (d, 2H, J = 15.8 Hz, H3), 7.59 (d, 2H, J = 15.8 Hz, H3), 9.64 (s, 4H, OH); ^{13}C NMR (DMSO-d_6): δ (ppm) 55.7 (C10), 59.8 (C11), 62.7 (C12), 111.2 (C9), 113.9 (C2), 114.1 (C2), 115.5 (C6), 123.5 (C5), 125.5 (C4), 145.4 (C3), 145.7 (C3), 147.9 (C8), 149.5 (C7), 166.4 (C1).

Alkylation reaction using iodopentane to synthesize M-PA-1. Tri-functional monomer M-1 (1 eq., 0.33 g, 0.53 mmol) and K_2CO_3 (4.5 eq., 0.33 g, 2.39 mmol) were dissolved in anhydrous DMF (1.5 M) under N_2. After 10 min, 1-iodopentane (4.5 eq., 312 μL, 2.39 mmol) was added and the reaction was stirred at overnight room temperature under N_2. The reaction mixture was extracted with dichloromethane and water, the organic layer was dried over anhydrous $MgSO_4$, filtered and concentrated *in vacuo* to afford the alkylated tri-functional monomer M-PA-1 (0.37 g, 0.44 mmol, 84% yield). ^{1}H NMR in DMSO-d_6 is given in Figure S1; ^{13}C NMR in DMSO-d_6 is given in Figure S2.

Alkylation reaction using iodopentane to synthesize M-PA-2. Tri-functional monomer M-2 (1 eq., 0.14 g, 0.17 mmol) and K_2CO_3 (4.5 eq., 0.10 g, 0.77 mmol) were dissolved in anhydrous DMF (1.5 M) under N_2. After 10 min, 1-iodopentane (4.5 eq., 100 μL, 0.77 mmol) was added and the reaction was stirred at overnight room temperature under N_2. The reaction mixture was extracted with dichloromethane and water, the organic layer was dried over anhydrous $MgSO_4$, filtered and concentrated *in vacuo* to afford the alkylated tri-functional monomer M-PA-2 (0.17 g, 0.15 mmol, 89% yield). ^{1}H NMR in DMSO-d_6 is given in Figure S3; ^{13}C NMR in DMSO-d_6 is given in Figure S4.

Synthesis of tri-functional monomer M-PA-3 using 3,4-dihydroxybenzaldehyde. Tris-*O*-malonate mono glycerol (1eq., 2.87 g, 8.19 mmol), 3,4-dihydroxybenzaldehyde (3 eq., 3.40 g, 24.58 mmol), aniline (0.3 eq., 224 μL, 2.46 mmol) were dissolved in pyridine and stirred together at 60 °C overnight. The reaction mixture was extracted with ethyl acetate and HCl 1M, the organic layer was dried over anhydrous $MgSO_4$, filtered and concentrated *in vacuo*. The crude product was then purified by column chromatography using ethyl acetate/cyclohexane (70/30) as an eluant to afford M-PA-3 monomer (2.52 g, 4.4 mmol, 53%). ^{1}H NMR in DMSO-d_6 is given in Figure S5.

Synthesis of hexa-functional monomer M-PA-4 using 3,4-dihydroxybenzaldehyde. Tris-*O*-malonate dipentaerythritol (1eq., 2.87 g, 3.73 mmol), 3,4-dihydroxybenzaldehyde (6 eq., 3.09 g, 22.38 mmol), aniline (0.6 eq., 204 μL, 2.24 mmol) were dissolved in pyridine and stirred together at 60 °C overnight. The reaction mixture was extracted with ethyl acetate and HCl 1M, the organic layer was dried over anhydrous $MgSO_4$, filtered and concentrated *in vacuo*. The crude product was then purified by column chromatography using ethyl acetate/cyclohexane as an eluant to afford M-PA-4 monomer (2.47 g, 2.0 mmol, 54%). ^{1}H NMR in DMSO-d_6 is given in Figure S6.

Alkylation reaction using iodopropane to synthesize M-PA-5. Tri-functional monomer M-PA-3 (1 eq., 0.62 g, 1.1 mmol) and K_2CO_3 (9 eq., 1.37 g, 9.90 mmol) were dissolved in anhydrous DMF (1.5 M) under N_2. After 10 min, 1-iodopropane (9 eq., 962 μL, 9.90 mmol) was added and the reaction was stirred at overnight room temperature under N_2. The reaction mixture was extracted with dichloromethane and water, the organic layer was dried over anhydrous $MgSO_4$, filtered and concentrated *in vacuo* to afford the alkylated tri-functional monomer M-PA-5 (0.81 g, 0.97 mmol, 88% yield). ^{1}H NMR in DMSO-d_6 is given in Figure S7.

Alkylation reaction using iodopentane to synthesize M-PA-6. Tri-functional monomer M-PA-3 (1 eq., 0.27 g, 0.46 mmol) and K_2CO_3 (9 eq., 0.57 g, 4.14 mmol) were dissolved in anhydrous DMF (1.5 M) under N_2. After 10 min, 1-iodopentane (9 eq., 540 μL, 4.14 mmol) was added and the reaction was stirred at overnight room temperature under N_2. The reaction mixture was extracted with dichloromethane and water, the organic layer was dried over anhydrous $MgSO_4$, filtered and concentrated *in vacuo* to afford the alkylated tri-functional monomer M-PA-6 (0.38 g, 0.38 mmol, 83% yield). ^{1}H NMR in DMSO-d_6 is given in Figure S8.

Formation of the crosslinked polymer by [2+2] cycloaddition reaction. The photo-responsive multi-functional monomers were dissolved in ethyl acetate and coated over glass/quartz slides using a spin coater. The slides were then placed inside the CL-1000L UV crosslinker and irradiated with 365 nm UV light to form the crosslinked polymer. The photo-reversible reaction (decrosslinking) was carried out in the CL-1000 UV crosslinker with 254 nm UV irradiation. The extent of crosslinking and decrosslinking was analyzed with UV-Vis spectroscopy.

Crosslinking extent was calculated using the UV-Vis absorption spectra at 327 nm as follows:

$$\frac{(\text{Initial absorption} - \text{absorption after irradiation})}{\text{Initial absorption}} \text{ x } 100\%$$

The extent of decrosslinking was calculated as follows:

$$\frac{\text{Absorption at 327 nm after irradiation}}{\text{Initial absorption at 327 nm}} \text{ x } 100\%$$

Statistics

All adhesive strength measurements were performed with n ≥ 2 or 3 data points. The experimental data collected against the design of experiments was analyzed by Response Surface Methodology (RSM).

Author Contributions

K.S. and F.A. contributed to the project idea and design. P.S.R. conducted all the experiments and characterizations and structured the manuscript. K.S., F.A. and G.G. provided critical suggestions during the project, helped with the execution strategies and provided comments and feedback to improve the manuscript writing. M.M.M. helped with the Design of Experiments and statistical analysis of the obtained results. A.P. provided critical comments and suggestions for the improvement of the manuscript and is assisting with future work on this project.

Conflicts of interest

There are no conflicts to declare.

Acknowledgments

The authors are grateful for the financial support provided by ARC Research Hub for Processing Advanced Lignocellulosics (PALS) IH170100020 and Monash University. K.S. acknowledges support from JSPS KAKENHI Grant-in-Aid for Scientific Research(B) JP22H02121. A.P., K.S. and G.G. are also thankful for the support of the Australian Research Council Industrial Transformation Training Centre (Green Chemistry in Manufacturing, project number IC190100034) funded by the Australian Government. M.M.M. and F.A. are grateful to Grand Reims, Département de la Marne and Région Grand Est for the financial support.

References

1. Nanayakkara, S.; Patti, A. F.; Saito, K., Chemical depolymerization of lignin involving the redistribution mechanism with phenols and repolymerization of depolymerized products. *Green Chemistry* **2014,** *16* (4), 1897-1903.
2. Upton, B. M.; Kasko, A. M., Strategies for the conversion of lignin to high-value polymeric materials: review and perspective. *Chemical reviews* **2016,** *116* (4), 2275-2306.
3. Meng, Q.; Yan, J.; Wu, R.; Liu, H.; Sun, Y.; Wu, N.; Xiang, J.; Zheng, L.; Zhang, J.; Han, B., Sustainable production of benzene from lignin. *Nature Communications* **2021,** *12* (1), 1-12.
4. Bruijnincx, P. C.; Weckhuysen, B. M., Lignin up for break-down. *Nature chemistry* **2014,** *6* (12), 1035-1036.
5. Mahajan, J. S.; O'Dea, R. M.; Norris, J. B.; Korley, L. T.; Epps III, T. H., Aromatics from lignocellulosic biomass: A platform for high-performance thermosets. *ACS Sustainable Chemistry & Engineering* **2020,** *8* (40), 15072-15096.
6. Engelen, S.; Wróblewska, A. A.; De Bruycker, K.; Aksakal, R.; Ladmiral, V.; Caillol, S.; Du Prez, F. E., Sustainable design of vanillin-based vitrimers using vinylogous urethane chemistry. *Polymer Chemistry* **2022,** *13* (18), 2665-2673.
7. Bass, G. F.; Epps, T. H., Recent developments towards performance-enhancing lignin-based polymers. *Polymer Chemistry* **2021,** *12* (29), 4130-4158.
8. Parkatzidis, K.; Boner, S.; Wang, H. S.; Anastasaki, A., Photoinduced Iron-Catalyzed ATRP of Renewable Monomers in Low-Toxicity Solvents: A Greener Approach. *ACS Macro Letters* **2022,** *11* (7), 841-846.
9. Kaur, G.; Johnston, P.; Saito, K., Photo-reversible dimerisation reactions and their applications in polymeric systems. *Polymer Chemistry* **2014,** *5* (7), 2171-2186.
10. Hughes, T.; Simon, G.; Saito, K., Chemistries and capabilities of photo-formable and photoreversible crosslinked polymer networks. *Materials Horizons* **2019,** *6* (9), 1762-1773.
11. Abdallh, M.; Yoshikawa, C.; Hearn, M. T.; Simon, G. P.; Saito, K., Photoreversible smart polymers based on 2π+ 2π cycloaddition reactions: nanofilms to self-healing films. *Macromolecules* **2019,** *52* (6), 2446-2455.
12. Hughes, T.; Simon, G.; Saito, K., Photocuring of 4-arm coumarin-functionalised monomers to form highly photoreversible crosslinked epoxy coatings. *Polymer Chemistry* **2019,** *10* (17), 2134-2142.
13. Hughes, T.; Simon, G.; Saito, K., Improvement and tuning of the performance of light-healable polymers by variation of the monomer content. *Polymer Chemistry* **2018,** *9* (47), 5585-5593.
14. Boga, K.; Patti, A. F.; Warner, J. C.; Simon, G. P.; Saito, K., Sustainable Light-Stimulated Synthesis of Cross-Linked Polymer Microparticles. *Macromolecular Chemistry and Physics* **2022**, 2100493.
15. Song, F.; Li, Z.; Jia, P.; Zhang, M.; Bo, C.; Feng, G.; Hu, L.; Zhou, Y., Tunable "soft and stiff", self-healing, recyclable, thermadapt shape memory biomass polymers based on multiple hydrogen bonds and dynamic imine bonds. *Journal of Materials Chemistry A* **2019,** *7* (21), 13400-13410.
16. Zhou, Y.; Chen, M.; Ban, Q.; Zhang, Z.; Shuang, S.; Koynov, K.; Butt, H.-J. r.; Kong, J.; Wu, S., Light-switchable polymer adhesive

based on photoinduced reversible solid-to-liquid transitions. *ACS Macro Letters* **2019,** *8* (8), 968-972.
17. Wang, Z.; Guo, L.; Xiao, H.; Cong, H.; Wang, S., A reversible underwater glue based on photo-and thermo-responsive dynamic covalent bonds. *Materials Horizons* **2020,** *7* (1), 282-288.
18. Gately, T. J.; Li, W.; Mostafavi, S. H.; Bardeen, C. J., Reversible Adhesion Switching Using Spiropyran Photoisomerization in a High Glass Transition Temperature Polymer. *Macromolecules* **2021,** *54* (20), 9319-9326.
19. Liu, W.; Fang, C.; Chen, F.; Qiu, X., Strong, Reusable, and Self-Healing Lignin-Containing Polyurea Adhesives. *ChemSusChem* **2020,** *13* (17), 4691-4701.
20. Wang, S.; Shuai, L.; Saha, B.; Vlachos, D. G.; Epps III, T. H., From tree to tape: direct synthesis of pressure sensitive adhesives from depolymerized raw lignocellulosic biomass. *ACS central science* **2018,** *4* (6), 701-708.
21. Droesbeke, M. A.; Aksakal, R.; Simula, A.; Asua, J. M.; Du Prez, F. E., Biobased acrylic pressure-sensitive adhesives. *Progress in Polymer Science* **2021,** *117*, 101396.
22. Liu, Z.; Liu, T.; Li, Y.; Zhang, X.; Xu, Y.; Li, J.; Gao, Q., Performance of soybean protein adhesive cross-linked by lignin and cuprum. *Journal of Cleaner Production* **2022,** *366*, 132906.
23. Wang, W.; Wang, F.; Zhang, C.; Tang, J.; Zeng, X.; Wan, X., Versatile value-added application of hyperbranched lignin derivatives: Water-resistance adhesive, UV protection coating, self-healing and skin-adhesive sensing. *Chemical Engineering Journal* **2021,** *404*, 126358.
24. Lendlein, A.; Jiang, H.; Jünger, O.; Langer, R., Light-induced shape-memory polymers. *Nature* **2005,** *434* (7035), 879-882.
25. Li, X.; Cui, J.; Zhang, W.; Huang, J.; Li, W.; Lin, C.; Jiang, Y.; Zhang, Y.; Li, G., Controllable photo-switching of cinnamate-based photonic films with remarkable stability. *Journal of Materials Chemistry* **2011,** *21* (44), 17953-17959.
26. Shi, D.; Matsusaki, M.; Kaneko, T.; Akashi, M., Photo-cross-linking and cleavage induced reversible size change of bio-based nanoparticles. *Macromolecules* **2008,** *41* (21), 8167-8172.
27. Du, H.; Zhang, J., The synthesis of poly (vinyl cinnamates) with light-induced shape fixity properties. *Sensors and Actuators A: Physical* **2012,** *179*, 114-120.
28. Oya, N.; Sukarsaatmadja, P.; Ishida, K.; Yoshie, N., Photoinduced mendable network polymer from poly (butylene adipate) end-functionalized with cinnamoyl groups. *Polymer journal* **2012,** *44* (7), 724-729.
29. Kuang, G.-C.; Ji, Y.; Jia, X.-R.; Li, Y.; Chen, E.-Q.; Zhang, Z.-X.; Wei, Y., Photoresponsive organogels: an amino acid-based dendron functionalized with p-nitrocinnamate. *Tetrahedron* **2009,** *65* (17), 3496-3501.
30. Russell, A. J.; Beckman, E. J.; Andreopoulos, F. M.; Wagner, W. R., Polymers for reversible photoinduced sol gel transitions. US Pat., 5,990,193, 1999.
31. Roy, P. S.; Mention, M. M.; Turner, M. A.; Brunissen, F.; Stavros, V. G.; Garnier, G.; Allais, F.; Saito, K., Bio-based photo-reversible self-healing polymer designed from lignin. *Green Chemistry* **2021,** *23* (24), 10050-10061.
32. Michal, B. T.; Spencer, E. J.; Rowan, S. J., Stimuli-responsive reversible two-level adhesion from a structurally dynamic shape-memory polymer. *ACS applied materials & interfaces* **2016,** *8* (17), 11041-11049.
33. Fadlallah, S.; Roy, P. S.; Garnier, G.; Saito, K.; Allais, F., Are lignin-derived monomers and polymers truly sustainable? An in-depth green metrics calculations approach. *Green Chemistry* **2021,** *23* (4), 1495-1535.
34. Roy, P. S.; Garnier, G.; Allais, F.; Saito, K., Effective lignin utilization strategy: major depolymerization technologies, purification process and production of valuable material. *Chemistry Letters* **2021,** *50* (6), 1123-1130.
35. Albarrán-Velo, J.; López-Iglesias, M.; Gotor, V.; Gotor-Fernández, V.; Lavandera, I., Synthesis of nitrogenated lignin-derived compounds and reactivity with laccases. Study of their application in mild chemoenzymatic oxidative processes. *RSC advances* **2017,** *7* (80), 50459-50471.
36. Pagliaro, M.; Ciriminna, R.; Kimura, H.; Rossi, M.; Della Pina, C., From glycerol to value-added products. *Angewandte Chemie International Edition* **2007,** *46* (24), 4434-4440.
37. Calvo-Flores, F. G.; Dobado, J. A., Lignin as renewable raw material. *ChemSusChem* **2010,** *3* (11), 1227-1235.
38. Kinloch, A., The science of adhesion. *Journal of materials science* **1980,** *15* (9), 2141-2166.
39. Brockmann, W.; Geiß, P. L.; Klingen, J.; Schröder, K. B., *Adhesive bonding: materials, applications and technology*. John Wiley & Sons: 2008.
40. Hatipoglu, A.; Vione, D.; Yalçın, Y.; Minero, C.; Çınar, Z., Photo-oxidative degradation of toluene in aqueous media by hydroxyl radicals. *Journal of Photochemistry and Photobiology A: Chemistry* **2010,** *215* (1), 59-68.
41. Zhang, D.; Gong, C.; Wang, J.; Mu, C.; Wang, W.; Zhang, X., Beyond lipid peroxidation: Distinct mechanisms observed for POPC and POPG oxidation initiated by UV-enhanced Fenton reactions at the air–water interface. *Journal of Mass Spectrometry* **2021,** *56* (4), e4626.
42. Tanaka, H.; Honda, K., Photoreversible reactions of polymers containing cinnamylideneacetate derivatives and the model compounds. *Journal of Polymer Science: Polymer Chemistry Edition* **1977,** *15* (11), 2685-2689.
43. Meredith, H. J.; Jenkins, C. L.; Wilker, J. J., Enhancing the adhesion of a biomimetic polymer yields performance rivaling commercial glues. *Advanced functional materials* **2014,** *24* (21), 3259-3267.
44. Bala, N.; Kamaruddin, I.; Napiah, M.; Sutanto, M. H., Polymer nanocomposite-modified asphalt: characterisation and optimisation using response surface methodology. *Arabian Journal for Science and Engineering* **2019,** *44* (5), 4233-4243.
45. Wang, Y.-Z.; Li, L.; Du, F.-S.; Li, Z.-C., A facile approach to catechol containing UV dismantlable adhesives. *Polymer* **2015,** *68*, 270-278.